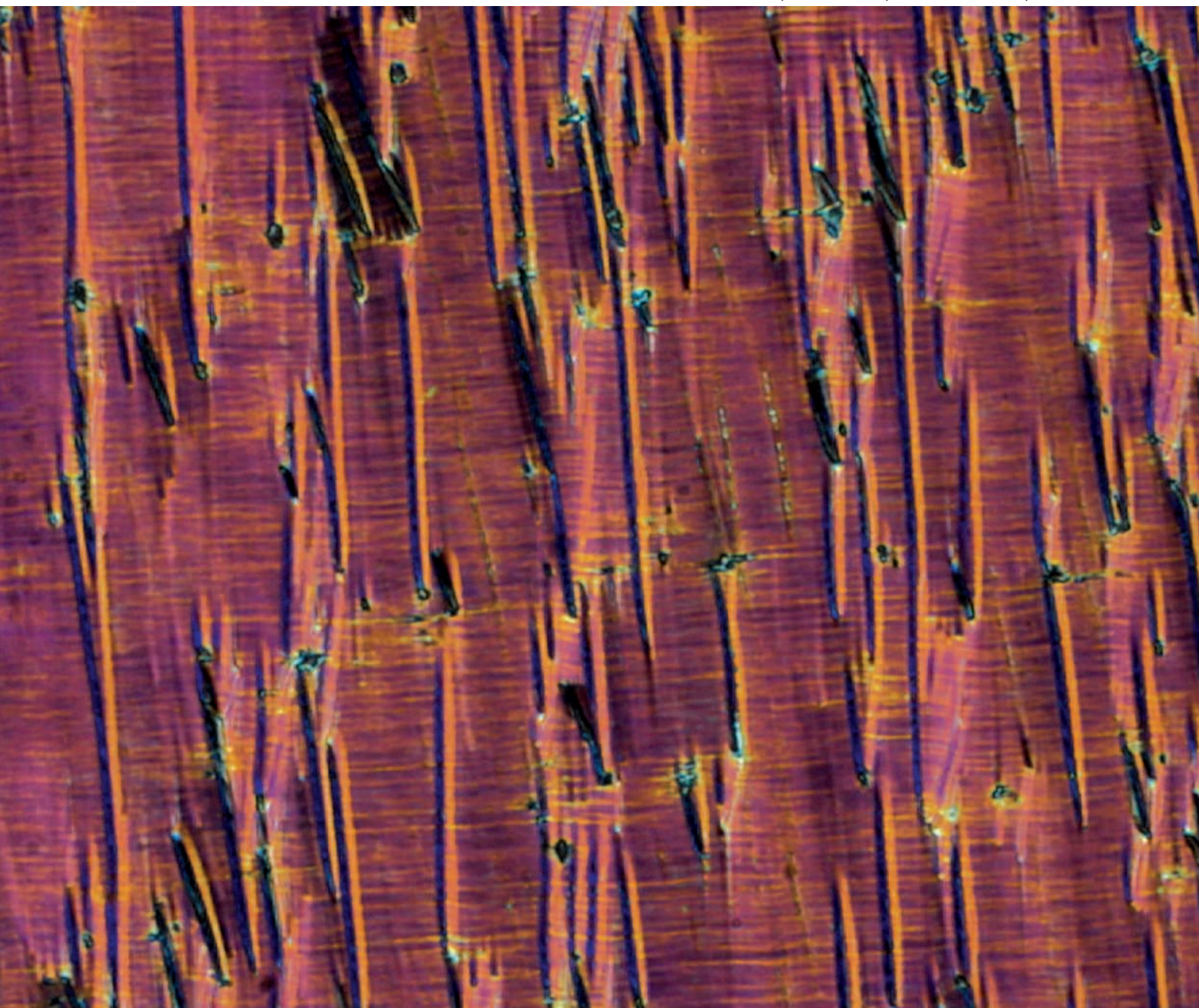


# Chem Soc Rev

Chemical Society Reviews

[www.rsc.org/chemsocrev](http://www.rsc.org/chemsocrev)

Volume 36 | Number 12 | December 2007 | Pages 1845–2128



ISSN 0306-0012

RSC Publishing

**TUTORIAL REVIEW**

Takashi Kato, Yuki Hirai, Suguru Nakaso and Masaya Moriyama  
Liquid-crystalline physical gels

# Liquid-crystalline physical gels

Takashi Kato,\* Yuki Hirai, Suguru Nakaso and Masaya Moriyama†

Received 21st July 2007

First published as an Advance Article on the web 3rd September 2007

DOI: 10.1039/b612546h

Liquid-crystalline (LC) physical gels are a new class of dynamically functional materials consisting of liquid crystals and fibrous aggregates of molecules that are called “gelators”. Liquid-crystalline physical gels, which are macroscopically soft solids, exhibit induced or enhanced electro-optical, photochemical, electronic properties due to the combination of two components that form phase-separated structures. In this *tutorial review*, we describe the materials design and structure–property relationships of the LC physical gels. The introduction of self-assembled fibers into nematic liquid crystals leads to faster responses in twisted nematic (TN) mode and high contrast switching in light scattering mode. Furthermore, the LC physical gels can be exploited as a new type of materials for electro-optical memory. This function is achieved by the control of reversible aggregation processes of gelators under electric fields in nematic liquid crystals. Electronic properties such as hole mobilities are improved by the introduction of fibrous aggregates into triphenylene-based columnar liquid crystals. The incorporation of photochromic azobenzenes or electroactive tetrathiafulvalenes into the chemical structures of gelators leads to the preparation of ordered functional materials.

## 1 Introduction

### 1.1 Physical and chemical gels

Gelation of organic fluids and water has attracted a great deal of attention because it yields elastic soft materials,<sup>1–9</sup> which can be used as functional materials in a variety of fields. The formation of three-dimensional (3D) chemical or physical molecular networks in fluids leads to the fabrication of chemical and physical gels, respectively (Fig. 1a,b). The chemical gels

consisting of covalently-bonded 3D polymer networks and organic fluids or water have been intensively studied.<sup>1</sup> The physical gels comprise 3D fibrous aggregates of low-molecular-weight compounds.<sup>2–9</sup> The molecules that induce gelation are called “gelators”. Fibrous assembly of gelators is driven by non-covalent interactions such as hydrogen bonding,  $\pi$ – $\pi$  interactions. Some representative gelators are shown in Fig. 2. Compounds 1–5 form one-dimensional fibrous aggregates through hydrogen bonding interactions,<sup>6–8</sup> while compound 6 self-assembles through  $\pi$ – $\pi$  interactions.<sup>9</sup>

Department of Chemistry and Biotechnology, School of Engineering, The University of Tokyo, Hongo, Bunkyo-ku, Tokyo 113-8656, Japan. E-mail: kato@chiral.t.u-tokyo.ac.jp; Fax: +81-3-5841-8661

† Present address: Department of Applied Chemistry, Faculty of Engineering, Oita University.

### 1.2 Liquid crystals and their gels

Recently, gels of liquid crystals have been developed to obtain functional soft materials. Liquid crystals are ordered



Takashi Kato

Dr Takashi Kato received his PhD from the University of Tokyo in 1988 under the supervision of professor Toshiyuki Uryu. After postdoctoral research at Cornell University with Professor Jean M. J. Fréchet on supramolecular hydrogen-bonded liquid crystals, he joined the University of Tokyo. He is now a full professor of the University of Tokyo. His research highlights the development of self-assembled functional molecular materials including supramole-

cular liquid crystals, liquid-crystalline physical gels, low-dimensionally ion-conductive liquid crystals and organic/inorganic composites inspired by biomineralisation. He received the



Yuki Hirai

Chemical Society of Japan Award for Young Chemists (1993), the Sakurada Memorial Award (1993), the IBM Japan Science Prize (2003) and the Japan Society for the Promotion of Science (JSPS) Prize (2004). He has published 260 articles including original papers, reviews and chapters of books.

Yuki Hirai was born in 1981. He has been working with professor Takashi Kato since 2004 and received his MS degree from the University of Tokyo in 2006. Currently he is working on the development of functional liquid-crystalline physical gels as a PhD student at the University of Tokyo.

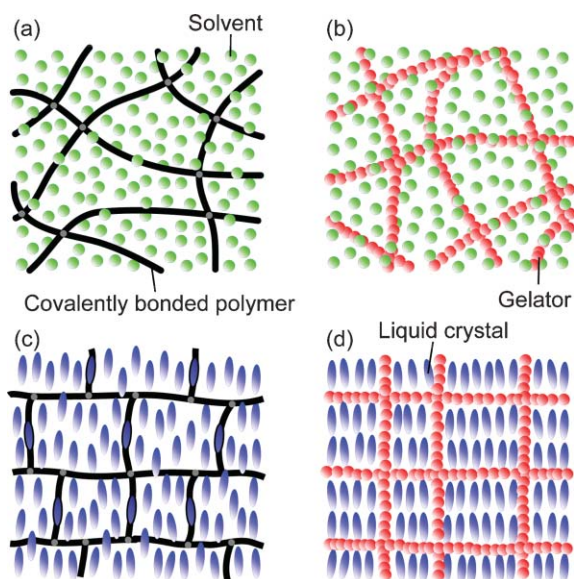


**Fig. 1** Schematic illustration of (a) chemical gels, (b) physical gels, (c) liquid-crystalline (LC) chemical gels and (d) LC physical gels.

fluids.<sup>10–14</sup> In the liquid-crystalline (LC) states, molecules form ordered and fluid states (Fig. 3). Typical LC molecules have rod-like and disk-like shapes (Fig. 4).<sup>10,11</sup> Rod-like compounds 7–9 exhibit nematic and smectic phases, while disk-like compound **10** shows a columnar phase. Liquid-crystalline rod-like molecules that show nematic phases in room temperature ranges have been applied for informational display of televisions and personal computers,<sup>11–13</sup> while aromatic  $\pi$ -conjugated disk-like molecules exhibiting columnar LC phases have been used for semiconductors.<sup>14</sup>

Liquid crystals are gelled with chemical or physical 3D network structures. The LC chemical gels<sup>10,15–18</sup> have been prepared by polymerisation of LC or non-LC monomers in liquid crystals (Fig. 1c).<sup>16–18</sup> Liquid-crystalline physical gels are obtained by the self-assembly of fibrous solid networks of gelators in liquid crystals (Fig. 1d, 5).<sup>19–45</sup> Liquid crystals become soft solids by gelation, keeping their stimuli-responsive properties. The formation of anisotropic phase-separated structures leads to the induction of new functions and the enhancement of the properties.<sup>29–45</sup> The LC physical gels are

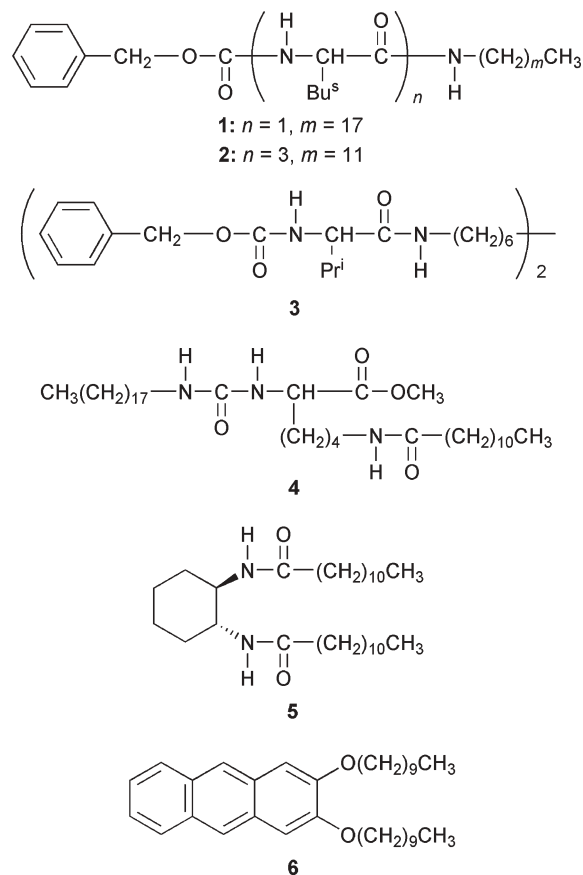


**Fig. 2** Molecular structures of several representative gelators.

normally formed by thermal processes, in which two independent transitions, the sol–gel transition of a gelator and the isotropic–anisotropic transition of a liquid crystal, are observed.<sup>23–28</sup>

## 2 Self-assembly of phase-separated structures

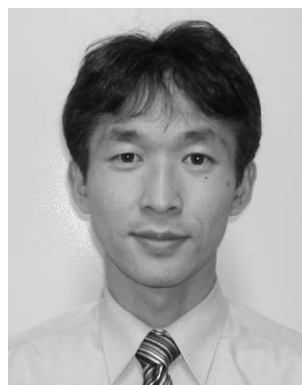
The phase-separated structures of LC physical gels are dependent on the order of sol–gel transition temperatures ( $T_{\text{sol-gel}}$ ) and isotropic–LC transition temperatures ( $T_{\text{iso-lc}}$ ).<sup>19,21,23–27</sup> Fig. 6 shows two types of phase transition



**Suguru Nakaso**

*Suguru Nakaso studied chemistry at the University of Tokyo, where he obtained his MS (2007) degrees at the Department of Chemistry and Biotechnology under the supervision of Professor Takashi Kato working on the development and alignment of electroactive supramolecular self-assembled nanofibers.*

*Masaya Moriyama received his PhD degree from the University of Tsukuba in 1998. After his postdoctoral*



**Masaya Moriyama**

*stay at the National Institute of Materials and Chemical Research (now National Institute of Advanced Industrial Science and Technology), he joined the group of Professor Takashi Kato at the University of Tokyo in 2001, where he studied functional liquid-crystalline physical gels. In 2006, he moved to Oita University as an associate professor. His research interests include functional soft materials such as photoresponsive liquid crystals.*

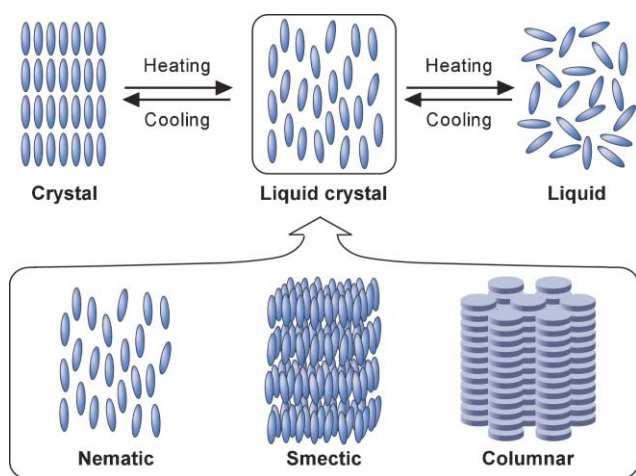


**Fig. 3** Schematic illustration of phase transition behaviour and the molecular order of liquid crystals.

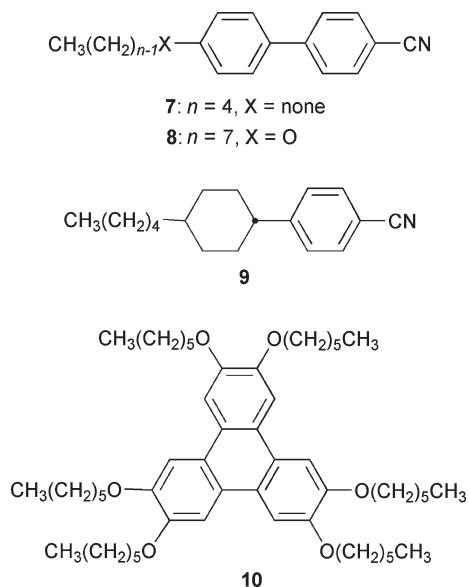


**Fig. 4** Molecular structures of several representative liquid crystals.

behaviour for the mixture of gelators and liquid crystals. Liquid-crystalline physical gels exhibit random or ordered phase-separated structures (Fig. 6c,e,f). When  $T_{\text{sol-gel}}$  is higher than  $T_{\text{iso-lc}}$  (Fig. 6, (a)  $\rightarrow$  (b)  $\rightarrow$  (c)), randomly dispersed fibrous networks of gelators are formed in the isotropic states of liquid crystals (Fig. 6, (a)  $\rightarrow$  (b)), resulting in the formation

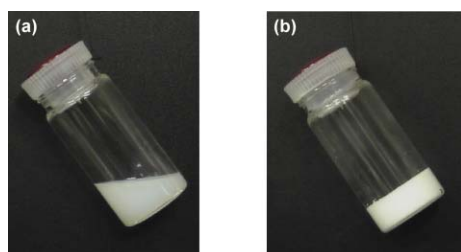


**Fig. 5** Photographs of (a) a nematic liquid crystal and (b) a nematic LC physical gel.

of isotropic gels (normal gels). On subsequent cooling, the LC gels are obtained by the isotropic–LC transitions of liquid crystals (Fig. 6, (b)  $\rightarrow$  (c)). These LC gels comprise random network structures of fibers. For example, gelator **1** forms random networks in nematic liquid crystal **7**.<sup>23</sup> The phase transition temperatures of the mixtures of **7** and **1** as a function of concentration of **1** on cooling are shown in Fig. 7a. For the mixture containing 4.0 wt% of **1**, the randomly dispersed networks of **1** are formed in the isotropic phase of **7** at 49 °C and the isotropic–nematic transition of **7** occurs in the networks at 33 °C.

In contrast, when  $T_{\text{iso-lc}}$  is higher than  $T_{\text{sol-gel}}$  (Fig. 6, (a)  $\rightarrow$  (d)  $\rightarrow$  (e),(f)), aligned fibers are formed by the template effects of oriented liquid crystals on rubbed polyimide-coated glass substrates (Fig. 6, (d)  $\rightarrow$  (e),(f)). The direction of the fiber alignment is dependent on the combination of the gelators and liquid crystals. For example, the alignment of fibers parallel to the long axis of rod-like LC molecules (Fig. 6e) is observed for a nematic liquid crystal containing **4**.<sup>30</sup> Fig. 7b shows the phase transition temperature of the mixture of **9** and **4** as a function of concentration of **4** on cooling. Fibrous self-assembly of **4** occurs in the nematic phase of **9** in the mixtures containing less than 1.2 wt% of **4**, resulting in the anisotropic fibrous aggregation. In this case, the anisotropic structures of LC media, *i.e.* the direction of the nematic director, determine the direction of the fibrous aggregation of **4**. Another case is LC physical gels consisting of **7** and **6**, in which the fibrous aggregation of **6** occurs in the nematic phase of **7**.<sup>27</sup> The fibers of **6** are formed in the direction perpendicular to the molecular long axis of **7** (Fig. 6f). The gelator is oriented in the direction parallel to the liquid crystals by the  $\pi$ – $\pi$  interactions between the liquid crystal and the  $\pi$ -conjugated gelator, leading to the formation of the anisotropic fibers perpendicular to the long axis of the liquid crystal. In this mixture, intermolecular interactions between the liquid crystal and the gelator seem to play important roles in the anisotropic self-assembly.

Smectic liquid crystals can also be used as templates for self-assembly of gelators (Fig. 8).<sup>26,28,42,43</sup> Because smectic liquid crystals have two-dimensionally ordered structures, there are two possibilities for the growth direction of the fibers: the direction of the long axis of the liquid crystals and the direction of the layered structures of smectic liquid crystals. When **1** is mixed with a commercially available liquid crystal, **SCE8** (Hoechst), the fibrous self-assembly of **1** occurs in the smectic A phase of **SCE8**. Fibrous aggregates of **1** grow in the direction perpendicular to the long axis of the liquid crystal, *i.e.* the direction of the smectic layer, in the mixtures of **SCE8** and **1**.<sup>26</sup> On the contrary, fibrous aggregates of **1** grow in the direction of the long axis of the liquid crystal in the mixtures of **8** and **1** containing 1.0 wt% of **1**, in which the nematic–smectic A transition temperature is 61 °C and the  $T_{\text{sol-gel}}$  is 47 °C.<sup>28</sup> These results can be attributed to the different degree of the ordering of smectic layered structures of liquid crystals. In the smectic liquid crystals with more distinct smectic layered structures, the fibrous aggregates may grow in the direction of the layer, while in the liquid crystals with less ordered smectic layered structures, fibrous aggregation may occur in the direction of long axis of liquid crystals.

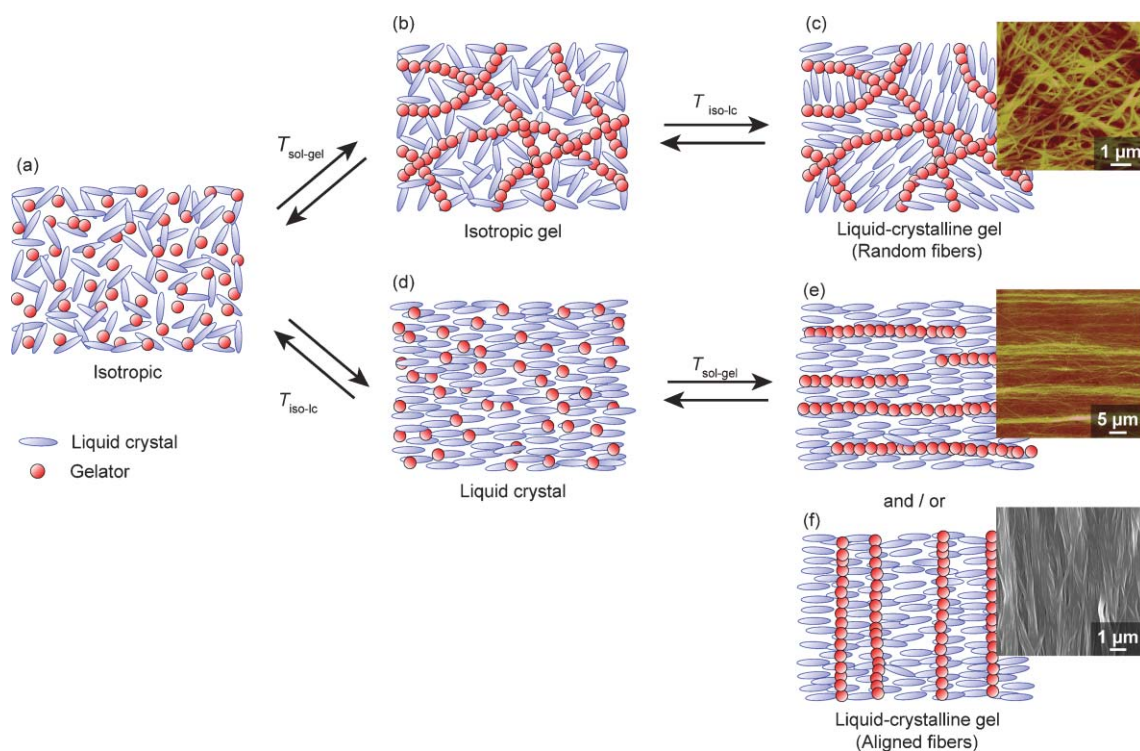


**Fig. 6** Schematic illustration of two types of thermoreversible structural changes of LC physical gels:  $T_{\text{sol-gel}} > T_{\text{iso-lc}}$  ((a)  $\rightarrow$  (b)  $\rightarrow$  (c));  $T_{\text{iso-lc}} > T_{\text{sol-gel}}$  ((a)  $\rightarrow$  (d)  $\rightarrow$  (e, f)). Inset of (c): AFM image of fibrous aggregates formed in gels consisting of **7** and **5**. Inset of (e, f): AFM image of fibrous aggregates of **4** formed in **9** (e) and SEM image of fibrous aggregates of **6** formed in **7** (f).

The control of the composite structures based on the choice of suitable components is important to give high functions such as electro-optical, photochemical and electronic properties to the LC physical gels described below.

### 3 Electro-optical properties

#### 3.1 Electro-optical effects in twisted nematic cells

Since the invention of twisted nematic (TN) mode for informational display in the 1970s, nematic liquid crystals have been developed significantly as electro-optical materials.<sup>10–13</sup> The nematic LC physical gel is a new class of electro-optical LC composites. They show improved electro-optical properties and novel switching modes when the phase-separated structures are tuned properly.<sup>29–35</sup>

Faster electro-optical switching of the nematic physical gels in TN cells has been achieved by introducing anisotropic self-assembled networks of gelators.<sup>29,30</sup> When the nematic LC physical gels consisting of **9** and 0.4 wt% of **4** is introduced into TN cells, fibrous aggregates of **4** is formed along the direction of the TN molecular orientation as shown in Fig. 9. Such template effects of the liquid crystals on self-assembly of gelators are described in Section 2. The nematic LC physical gel with oriented phase-separated structures in TN mode exhibits faster responses than the single component of the nematic liquid crystal. The rise times (the time period required for a 100–10% transmittance change by application of electric field) are improved from 17 ms to 7 ms by the introduction of aligned networks of gelators. Threshold voltages (the voltage

required for a 100–90% transmittance change) of the nematic gels and the liquid crystals alone are 0.7 V and 1.7 V, respectively (Fig. 10). The existence of anisotropic fibers of **4** may induce a metastable TN alignment state that leads to faster responses. Oriented fibrous aggregates do not exert effects on the long-range alignment of liquid crystals. As a result, relatively high light transmission, which reaches 88% of that observed for the TN cells of liquid crystals alone, is obtained for the LC physical gels with oriented networks.

#### 3.2 Electro-optical switching in light scattering mode

Liquid-crystalline physical gels with randomly dispersed networks of gelators are applicable to light-scattering electro-optical materials.<sup>31–34</sup> Liquid-crystalline composites such as polymer dispersed liquid crystal (PDLC) for light-scattering display materials have been intensely studied from the 1980s.<sup>46–48</sup> The formation of microphase-separated structures of polymers and LC micro-domains results in light scattering states due to the mismatch of refractive indices of the components. Light-scattering LC composites are expected to be of great potential for large area displays because of the efficient use of the incident light and simpler device structures. Liquid-crystalline physical gels are a new class of LC composites containing small amounts of additives (0.2 ~ 1.0 wt%) that induce light scattering states effectively.<sup>31,32</sup>

Nematic LC physical gels consisting of **7** and **2** exhibit electro-optical switching in the light scattering mode.<sup>31</sup> Fig. 11 shows electro-optical switching of the LC physical gels. On cooling the nematic gels consisting of **7** and 0.2 wt% of **2** from

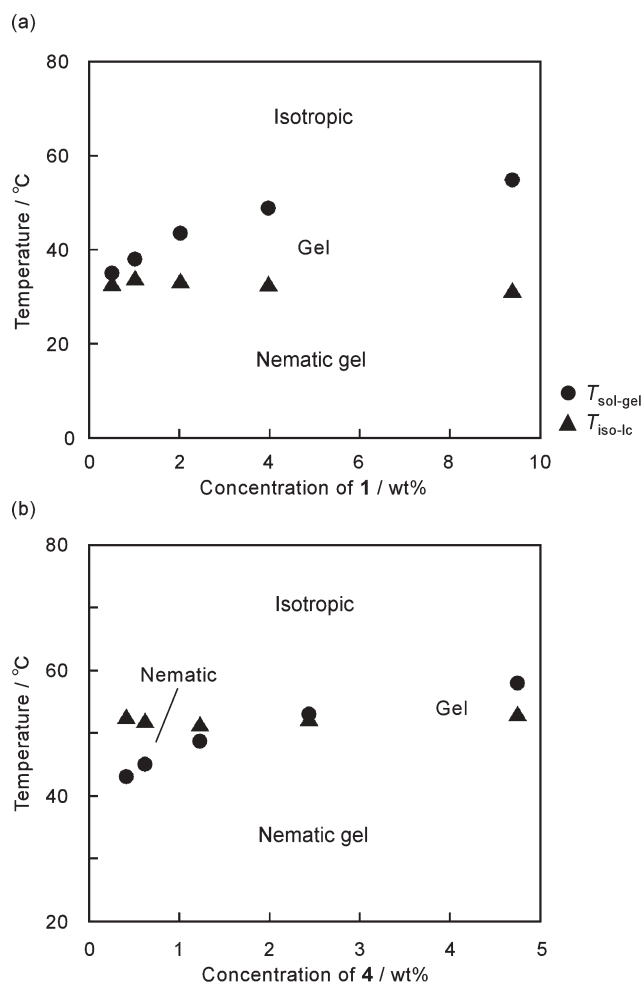


**Fig. 7** Phase transition behaviour of the mixtures of liquid crystals and gelators on cooling: (a) **7** and **1**; (b) **9** and **4**.

the isotropic state, randomly dispersed networks are formed in the isotropic phase of **7**. After the isotropic–LC transition of **7**, an LC polydomain with a size of 1–2  $\mu\text{m}$  is induced by finely dispersed fibrous networks of **2**. Liquid-crystalline physical gels with such polydomain structures exhibit light-scattering states (Fig. 11a). Upon application of an electric field, the LC molecules reorient in the direction of the electric field, resulting in the homeotropically aligned monodomain structures. The aligned monodomain states of LC physical gels transmit incident light (Fig. 11b). As shown in Fig. 12, switching contrast is very high reaching to 67 where the transmittance in electric field ON- and OFF-state is 94% and 1.4%, respectively. The nematic LC physical gels show reversible switching without significant hysteresis. The concentration of the additives that are needed to induce such high contrast is much lower than that for other light-scattering LC materials such as PDLC<sup>46–48</sup> and filled nematics.<sup>49</sup> It is due to the well-dispersed networks of fibrous aggregates in liquid crystals for LC physical gels. The rise and decay times for application and removal of the electric field of 100 V are 0.5 ms and 1.8 ms, respectively, that are comparable to those reported for liquid crystal–polymer composites. Although the non-covalent networks of gelators are generally stable for switching

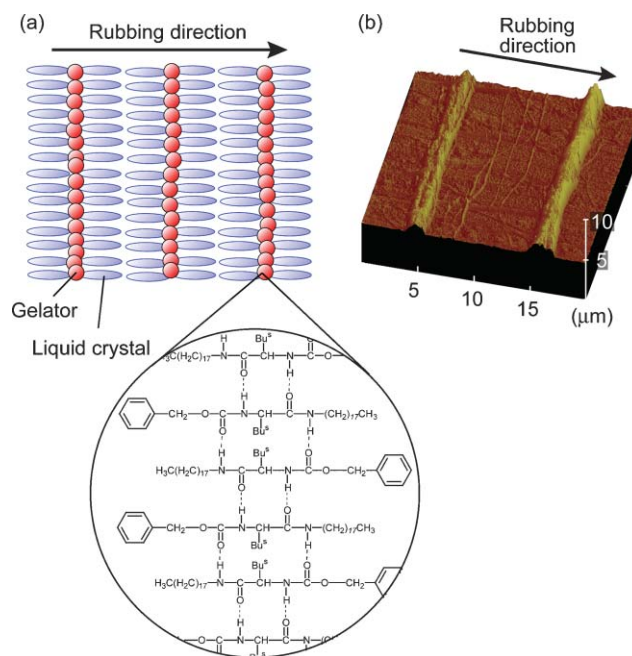


**Fig. 8** (a) Schematic illustration of anisotropically oriented fibers formed in the oriented smectic liquid crystals. (b) AFM image of the anisotropic fibers formed in the gels of SCE8 containing 1.0 wt% of **1**.

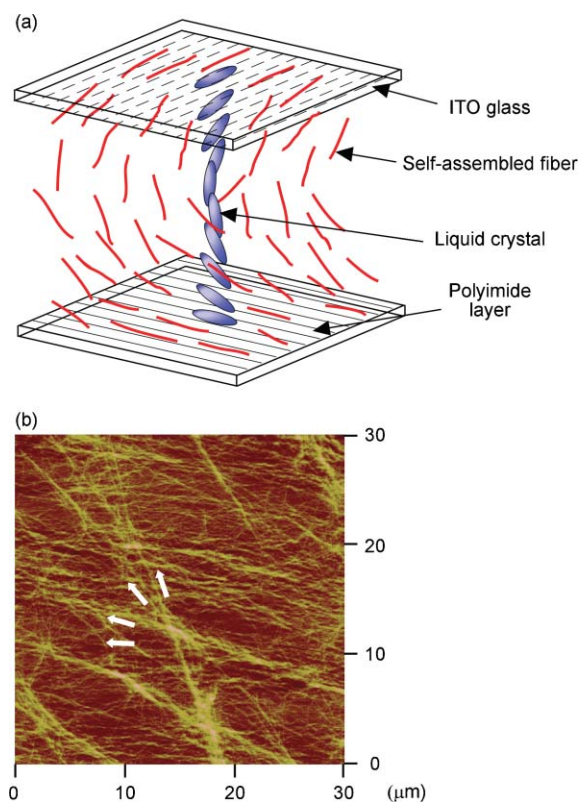


**Fig. 9** (a) Schematic illustration of twisted nematic (TN) cells with oriented fibrous networks. (b) AFM image of the fibrous aggregates of **4** obtained from the gels of **9** containing 0.4 wt% of **4** in 16  $\mu\text{m}$  thick TN cells. Reproduced with permission from ref. 30. Copyright 2003 Wiley-VCH.

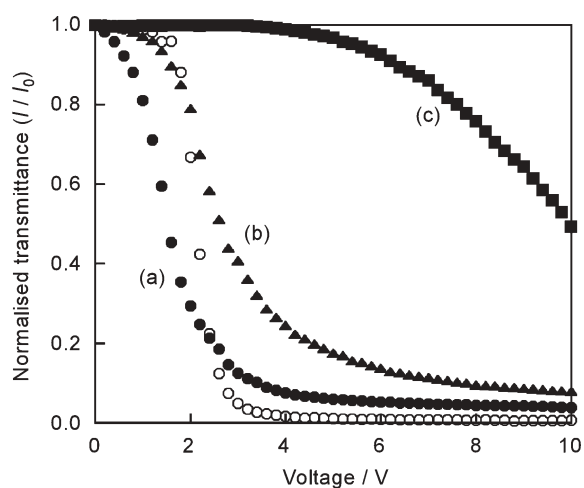


**Fig. 10** Relationship between transmittance and applied voltage for **9** (open circles) and the gels of **9** containing (a) 0.4 wt%, (b) 1.1 wt% and (c) 2.3 wt% of **4** in 16  $\mu\text{m}$  thick TN cells. Reproduced with permission from ref. 30. Copyright 2003 Wiley-VCH.

at voltages lower than about 40 V, the stability of the networks at higher voltages is not enough and should be improved.

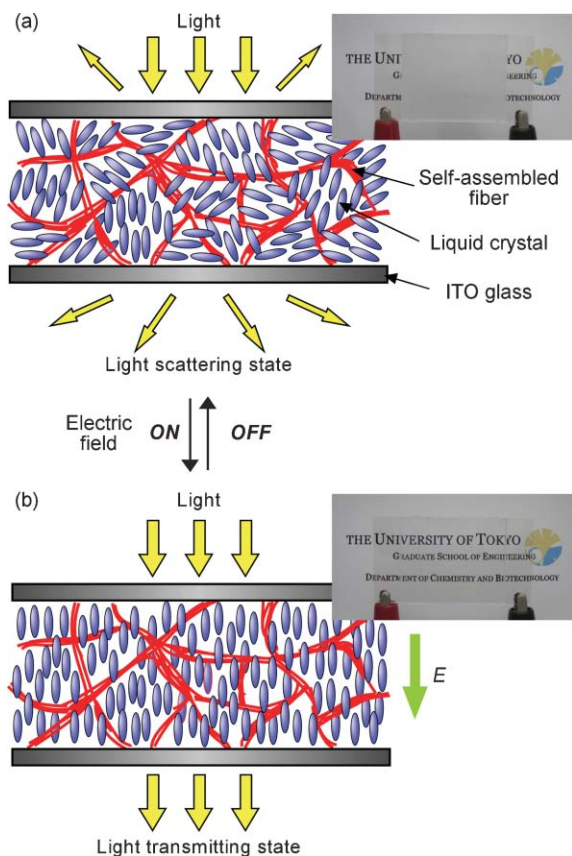


**Fig. 11** Schematic illustration of light-scattering electro-optical switching of nematic LC gels and the photographs of liquid crystal cells filled with LC physical gels consisting of **7** and **2**; (a) light scattering state (electric field OFF) and (b) light transmitting state (electric field ON).

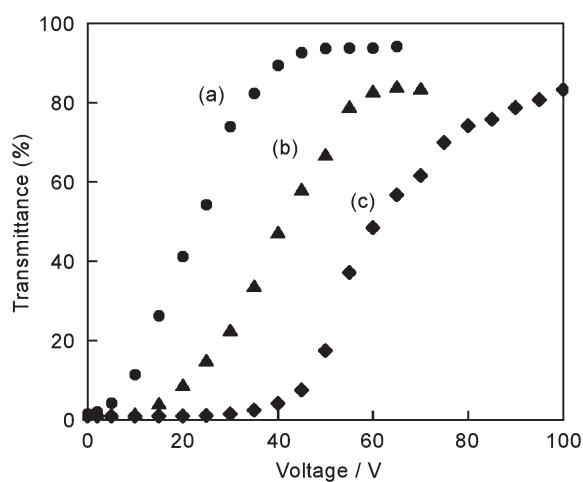


**Fig. 12** Relationship between transmittance and applied voltage for the gels of **7** containing (a) 0.2, (b) 0.5 and (c) 1.0 wt% of **2** in 16  $\mu\text{m}$  thick cells.

The electro-optical properties of LC physical gels can be tuned by chemical modification of the components, and changing the choice and the concentration of the gelators.<sup>31</sup> In the case of the gelators derived from L-isoleucine, **1** and **2**, increased number of amino acid moieties leads to stronger one-dimensional molecular association, resulting in the formation of LC physical gels with the finer dispersion and higher thermal stability of fibrous networks. Finely well-dispersed networks induce light scattering states effectively in the lower concentration of the gelator. They also contribute to the improvement of the electro-optical properties of LC physical gels such as threshold voltages and response times. The tuning of the concentration of gelators is also generally an effective way to improve the electro-optical properties. In the case of nematic LC physical gels consisting of **7** and **2**, preferable electro-optical switching both with higher contrast and lower driving voltage is achieved in the concentration of 0.2 wt% of **2** (Fig. 12). As the concentration of **2** is decreased to 0.2 wt%, higher transmittance in the ON-state and lower driving voltages are obtained, while the degree of light scattering in the electric field OFF-state remains relatively high. Use of liquid crystals with higher birefringence will also contribute to the further enhancement of light-scattering electro-optical properties of LC physical gels.

### 3.3 Bistable nematic liquid crystals with self-assembled fibers

A novel bistable electro-optical switching, which can be applicable for rewritable memory, is achieved by thermo-reversible formation of composite structures in the nematic gels under electric fields (Fig. 13).<sup>35</sup> Such dynamic electro-optical functions have not been attained in the conventional polymeric LC composites.

The nematic gels are obtained by mixing a room temperature nematic liquid crystal **E63** (Merck) and 1.0 wt% of **4**. These components have been chosen such that the  $T_{\text{iso-lc}}$  of liquid crystals is higher than the  $T_{\text{sol-gel}}$  of gelators. The orientation of the nematic liquid crystal is manipulated by external electric fields. The homeotropic monodomain state

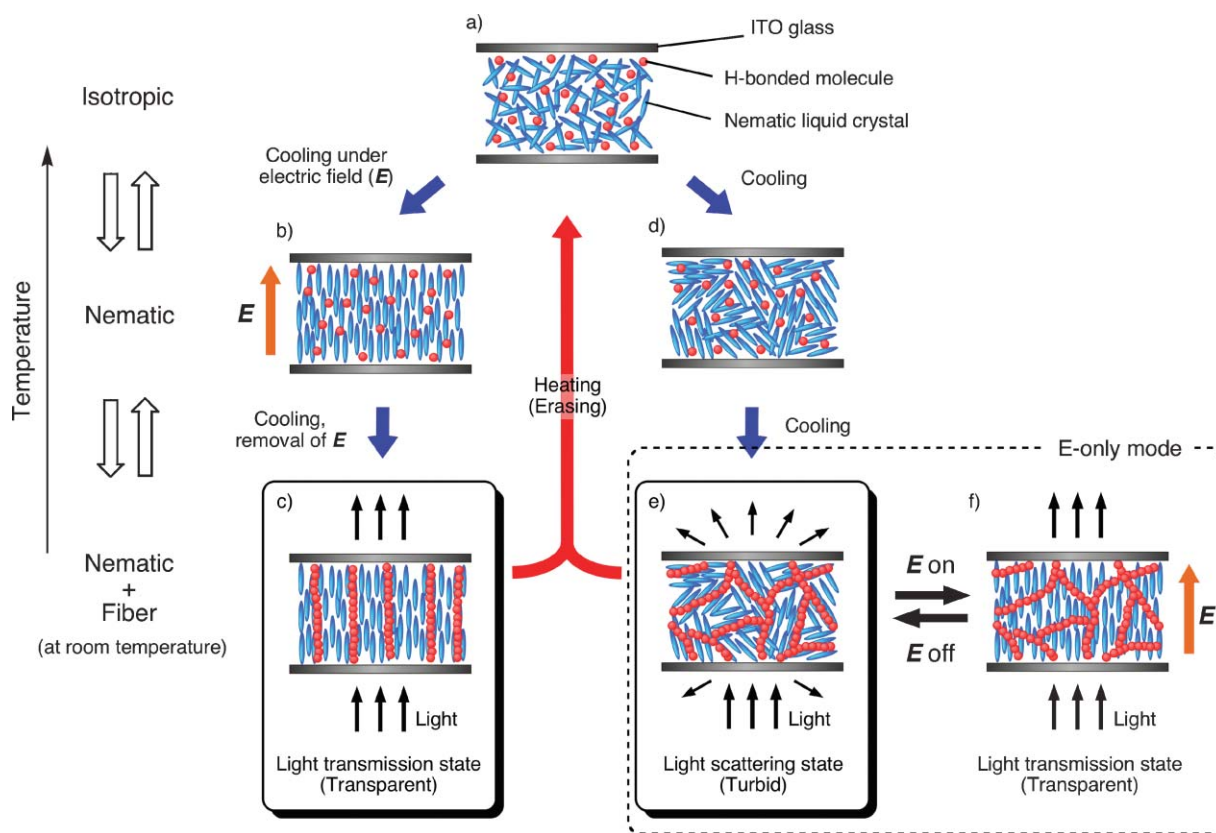


**Fig. 13** Schematic illustration of the bistable fixation of LC alignment through molecular self-organization process of liquid crystals and hydrogen-bonded molecules (a–e) and isothermal electro-optical switching (e, f; E-only mode). Reproduced with permission from ref. 35. Copyright 2005 Wiley-VCH.

(electric field ON) and the non-aligned polydomain state (electric field OFF) of the liquid crystal are fixed by self-assembled fibrous aggregates of the gelator. Fig. 13 shows bistable fixation of LC alignment in nematic LC physical gels. In the absence of electric fields, dispersed random networks of gelators are formed in the polydomain states of nematic liquid crystals on cooling from the isotropic state (Fig. 13, (a)  $\rightarrow$  (d)  $\rightarrow$  (e)). On the contrary, oriented fibrous aggregates of **4** are formed in the electrically aligned nematic phase upon cooling the mixture with an electric field applied (Fig. 13, (a)  $\rightarrow$  (b)  $\rightarrow$  (c)). The homeotropically aligned monodomain of liquid crystals is kept after the removal of an electric field because of the existence of aligned fibrous aggregates (Fig. 13c). After the formation of the fibrous aggregates at  $T_{\text{sol-gel}}$ , these two states (Fig. 13c,e) are equally stable at room temperature. The polydomain states formed without the electric field exhibit light scattering while the aligned monodomain states formed with the electric field are transparent. Such bistable structures with optical contrast can be applied to light-scattering memory materials. The formation processes of the bistable structure in the LC physical gels are fully reversible because the LC alignment is fixed by the self-assembled fibers. The images can be erased by heating the mixtures to the isotropic state where the hydrogen bonds of the gelator dissociate (Fig. 13, (c),(e)  $\rightarrow$  (a)). Then the image can be rewritten on cooling with the application of the electric field.

## 4 Photo-functions of LC physical gels

### 4.1 Photo-control of the structures of LC physical gels

The composite structures of LC physical gels can be changed by external stimuli such as light as well as thermal stimuli. If gelators have photoresponsive moieties, light stimuli can induce dynamic changes of anisotropic composite structures.<sup>36–39</sup> For example, the photoresponsive LC gels are obtained for the mixtures of nematic liquid crystal (**7**) and a hydrogen-bonded chiral gelator having photochromic azobenzene moieties (**11**) (Fig. 14, 15).<sup>36</sup> The LC mixtures containing **11** with *trans*-azobenzene moieties<sup>37</sup> form nematic LC gels at room temperature (Fig. 15, (a)  $\rightarrow$  (b)). Because the  $T_{\text{sol-gel}}$  is higher than the  $T_{\text{iso-lc}}$ , these nematic gels have microphase-separated structures comprising the randomly dispersed aggregates of **11**. When the nematic gels are exposed to UV light, structural changes can be induced by *trans*-to-*cis* photoisomerisation of the azobenzene moieties. The

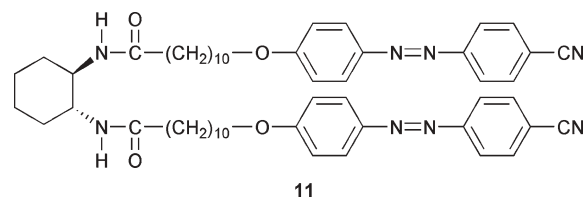


**Fig. 14** Molecular structure of a photoresponsive gelator.



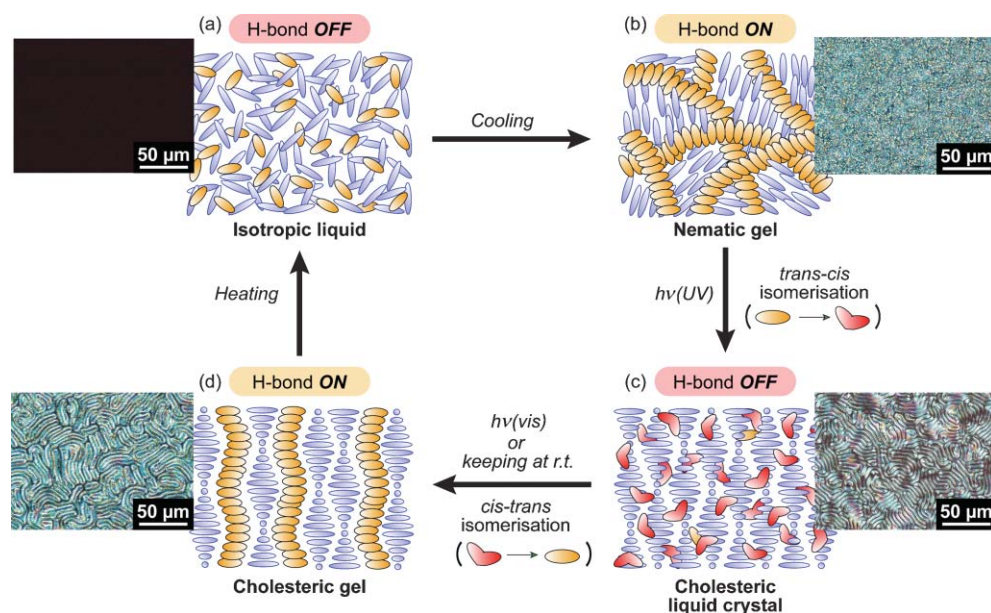


**Fig. 15** Optical polarised photomicrographs and schematic illustration of photo-induced structural changes in LC physical gels consisting of **7** containing 3 wt% of **11**: (a) isotropic liquid state at 120 °C; (b) nematic gel state at room temperature before UV irradiation; (c) cholesteric LC phase (LC sol state) at room temperature after UV irradiation (30 mW cm<sup>-2</sup>) of the nematic gels for 15 min; (d) cholesteric gel state at room temperature after keeping the cholesteric LC phase.

photoisomerisation causes the dissociation of hydrogen bonds and the chiral compound of **11** dissolves into the host nematic liquid crystal, resulting in the phase transition from the nematic gel states to the cholesteric LC sol states (Fig. 15, (b) → (c)). The cholesteric sol states are changed to the cholesteric gel states by the *cis*-to-*trans* back-isomerisation of the azobenzenes (Fig. 15, (c) → (d)). In this stage, the cholesteric molecular alignment should behave as a template for the aggregation of gelators. Both the nematic and the cholesteric gels are stable at room temperature and can be repeatedly produced by providing light stimuli and thermal treatments as shown in Fig. 15. The composite structural changes of discotic LC gels consisting of **11** and **10** are also induced by light stimuli.<sup>38</sup> Light-induced reorganisation of LC physical gels is also applicable to the formation of electrically switchable diffracting gratings.<sup>39</sup>

#### 4.2 Photopolymerisation of self-assembled fibers

The incorporation of a polymerisable group into a gelator has led to the preparation of a new type of smectic LC physical gels (Fig. 16 and 17).<sup>40</sup> Anisotropic fibrous aggregates are stabilised by photopolymerisation and resultant oriented microgrooves are formed on the substrate surface. These surface structures induce the orientation change of the LC molecules.

An L-isoleucine derivative with polymerisable methacryloyl moieties (**12**) is mixed with a smectic liquid crystal and a photoinitiator. The sol–gel transition occurs in the smectic A

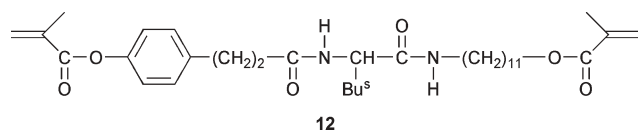


**Fig. 16** Molecular structure of a polymerisable gelator.

phase of the liquid crystal for the gels containing a small amount of photoinitiator on cooling. When the mixtures are introduced into the liquid-crystal cells coated with parallel-rubbed polyimide layers, the fibers comprising **12** grow in the homogeneously oriented smectic A phase of the liquid crystal (Fig. 17a). The growth direction of the fibers is perpendicular to the long axis of liquid crystal molecules, *i.e.* the direction of smectic layer. The anisotropic structures of the oriented fibers are effectively fixed and stabilised by photoinduced chemical crosslinking of the methacryloyl moieties of the gelator upon UV irradiation (Fig. 17b).

Polymerised anisotropic fibers affect the LC orientation. When the polymerised cell is heated to 100 °C, at which the LC component becomes isotropic, and subsequently cooled to room temperature, the liquid crystal is aligned along the groove structures of the polymerised fibers (Fig. 17c). The patterning of LC orientation is achieved by UV irradiation of the mixtures through photomasks (Fig. 17d). For the UV-exposed regions, the liquid crystal is aligned along the direction of the polymerised fibers, while the orientation along the rubbing direction is observed in the non-exposed regions.

#### 5 Liquid-crystalline semiconductor with self-assembled fibers

Discotic liquid crystals form organised columnar structures with stacked aromatic cores surrounded by insulating alkyl chains.<sup>10,14</sup> Resulting from such organised structures, the discotic liquid crystals can exhibit anisotropic carrier transport with higher mobility than conventional amorphous semiconductors.<sup>14</sup>

We have developed discotic LC physical gels by combining a hole transporting triphenylene derivative (**10**) and the hydrogen-bonded networks of gelator **3** (Fig. 18).<sup>41</sup> Compound **10**

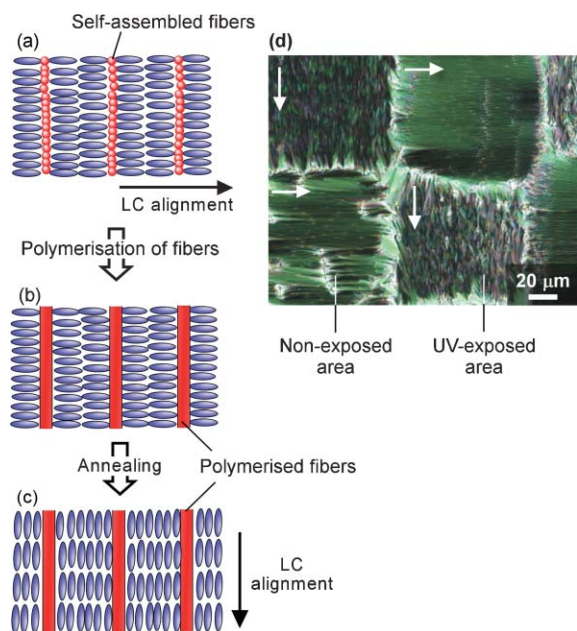


**Fig. 17** Schematic illustration (top view) of the alignment process of liquid crystals with fibrous materials at the substrate surfaces: (a) anisotropic fibers formed in liquid-crystal cells coated with rubbed polyimide surfaces; (b) photopolymerised oriented fibrous aggregates; (c) alignment of liquid-crystal molecules along the grooved structures of polymerised anisotropic fibers after thermal annealing. (d) Polarised optical photomicrograph of patterned liquid-crystal alignment formed by UV irradiation of the mixture of the liquid crystal, **12** and photoinitiator in parallel-rubbed cells through a checker-patterned photomask and subsequent thermal annealing.

shows a hexagonal columnar phase ( $\text{Col}_h$ ) between 98 °C and 54 °C on cooling. For the gels of **10** containing 3 wt% of **3**, the  $T_{\text{sol-gel}}$  and the  $T_{\text{iso-lc}}$  are 133 °C and 97 °C, respectively. On cooling the mixtures of **10** and **3**, the finely dispersed random networks of **3** are formed because the fibrous aggregation of **3**

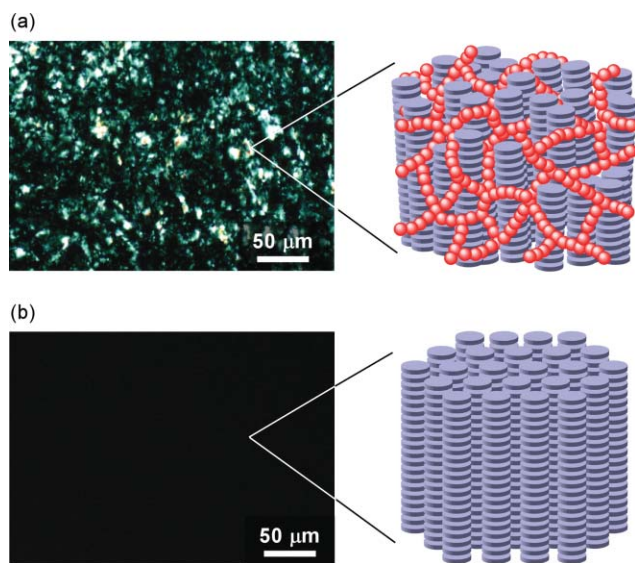


**Fig. 18** Polarised optical photomicrographs and schematic illustration of the structures of (a) the gels of **10** containing 3 wt% of **3** and (b) **10**.

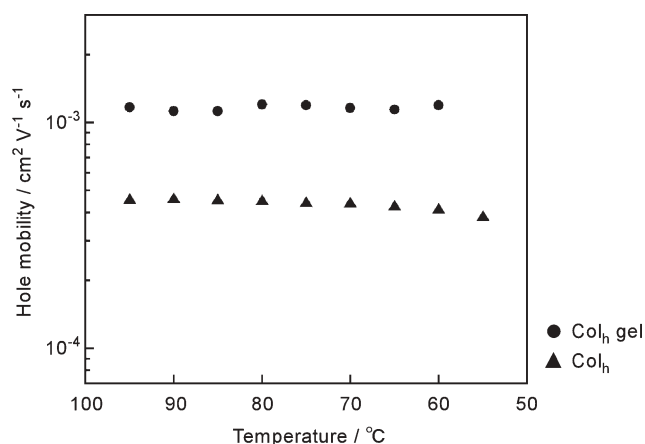


**Fig. 19** Temperature dependence of hole mobilities of **10** and the gels of **10** containing 3.0 wt% of **3**.

occurs in the isotropic phase of **10** (Fig. 18a). The  $\text{Col}_h$  gel states are obtained on further cooling. The fibers of **3** are ca. 40 nm in diameter and the networks form LC domains in the scale of several hundred nanometers.

Compound **10** alone shows almost perfect homeotropic alignment in the  $\text{Col}_h$  phase on the glass substrate as observed under a polarising microscope (Fig. 18b). On the contrary, the introduction of the fibrous networks of **3** induces partial disorder in the LC alignment of **10**. When the gels of **10** containing 3 wt% of **3** are observed under a polarising microscope on a glass substrate, the LC domains in the submicrometer scale is observed (Fig. 18a). This partial disorder in the LC alignment has a negative effect on the hole transport because holes can be trapped by such structural defects.

The hole mobilities of **10** alone and the discotic LC gels obtained by the time-of-flight method are compared in Fig. 19. The hole mobility of the **10** is  $4.5 \times 10^{-4} \text{ cm}^2 \text{V}^{-1} \text{s}^{-1}$  in the  $\text{Col}_h$  phase (75 °C) and agrees well with the values previously reported.<sup>50</sup> Interestingly, the hole mobility of the gels of **10** containing 3 wt% of **3** in the  $\text{Col}_h$  gel phase (75 °C) is  $1.2 \times 10^{-3} \text{ cm}^2 \text{V}^{-1} \text{s}^{-1}$  that is three times higher than that of the liquid crystal. It is noteworthy that the enhancement of hole mobilities are observed even though the LC alignment is partially disturbed by fibrous networks of **3** (Fig. 18). We assume that the finely dispersed networks of **3** effectively suppress the molecular fluctuation of **10** and enhance the degree of the columnar ordering, leading to the faster hole transport. Appropriate tuning of the microphase-separated structures of the discotic LC gels may contribute to the fabrication of a new class of organic electroactive materials. The present results suggest that well-tuned composite structures of molecular composites can enhance the properties of functional molecules.

## 6 Conductive self-assembled fibers

The introduction of electroactive moieties into the self-assembled fibers is one of important approaches toward molecular electronics (Fig. 20).<sup>42,43,51</sup> If the electroactive moieties stack in one dimensional order in liquid crystals, aligned molecular conductive wires can be obtained.

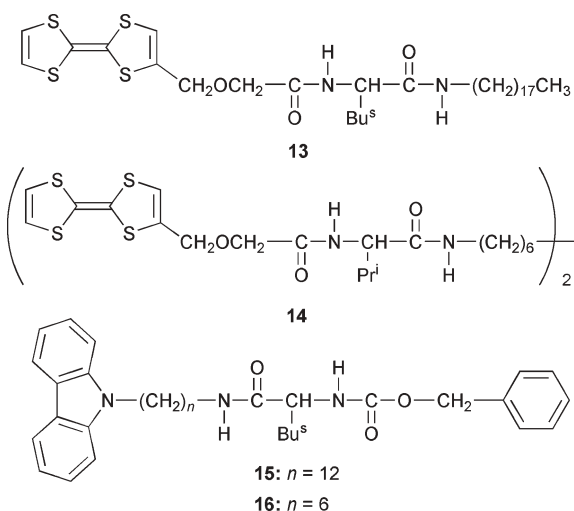


**Fig. 20** Molecular structures of gelators having electroactive moieties.

Tetrathiafulvalene (TTF) moieties have been introduced into the fibers. Intensive studies have focused on TTF for the preparation of conductive materials in bulk and thin film states.<sup>52,53</sup> Electroactive nanofibers have been formed by self-assembly of TTF derivatives **13** and **14** in liquid crystals. These derivatives were prepared by introducing the TTF moieties to the scaffold derived from amino acids such as L-isoleucine and L-valine whose derivatives function as gelators.<sup>6</sup> There are only a few examples of self-assembled fibers containing the TTF moieties.

Stable fibrous aggregates of these TTF derivatives are formed in liquid crystals, resulting in efficient gelation of these anisotropic solvents. In a smectic liquid crystal oriented parallel to the surface of the substrate, aligned fibrous aggregates are obtained (Fig. 21). The UV-vis spectra and X-ray diffraction patterns for the oriented fibrous aggregates indicate the stacking of the TTF moiety. The polarised IR spectra of the gel show that these compounds form intermolecular hydrogen bonds in the parallel  $\beta$ -sheet conformation and the hydrogen-bonded chains align along the fiber direction.

Iodine-doping of the fibrous aggregates have been carried out by exposure to iodine vapor in a sealed container. The UV-vis-NIR spectra for the fibrous aggregates show that immediately after iodine-doping, a new absorption band is observed at 850 nm, which indicates the formation of full CT state. When the sample is kept in air after exposure to iodine

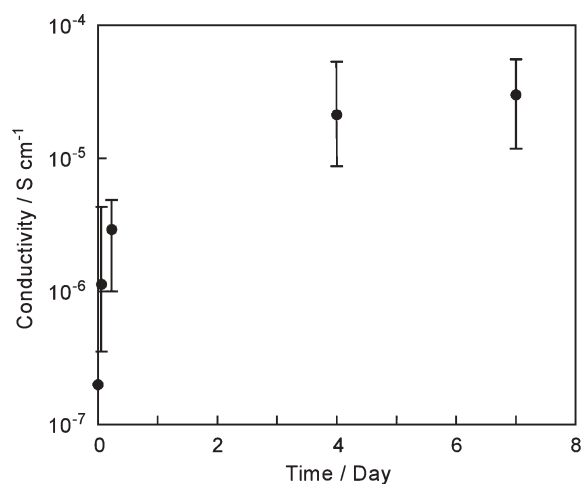


**Fig. 22** The electronic conductivities for the self-assembled fibers of **13** as a function of time period after iodine-doping.

vapor, gradual release of iodine occurs. The CT band at 850 nm becomes weaker in intensity, and a broad band appears at 2300 nm. The full CT state has changed to a more stable mixed-valence conducting state with gradual release of iodine over time.

The electronic conductivities of randomly dispersed fibrous aggregates of the TTF derivatives are shown in Fig. 22. The fibers in the neutral state before doping behave as insulator ( $\sigma < 3 \times 10^{-10} \text{ S cm}^{-1}$ ). The conductivity increases after iodine-doping for 2 min ( $\sigma = 2 \times 10^{-7} \text{ S cm}^{-1}$ ). The conductivity reaches a maximum at  $3 \times 10^{-5} \text{ S cm}^{-1}$  seven days after the exposure to iodine vapor. The fibers forming the CT states can function as conductive materials.

Carbazolyl moieties are known to exhibit photophysical properties such as photoconductivity.<sup>54</sup> The carbazole-containing gelators with an L-isoleucine scaffold (**15**, **16**) form one dimensional fibrous aggregates.<sup>43</sup> The carbazolyl moieties are stacked in the one dimensionally aligned fibers. Unidirectionally aligned fibers have been obtained in an oriented smectic liquid crystal. These fibers may be a good candidate for new electro-active materials.

## Conclusions

This review summarises the development of LC physical gels. The combination of liquid crystals and self-assembled fibers of

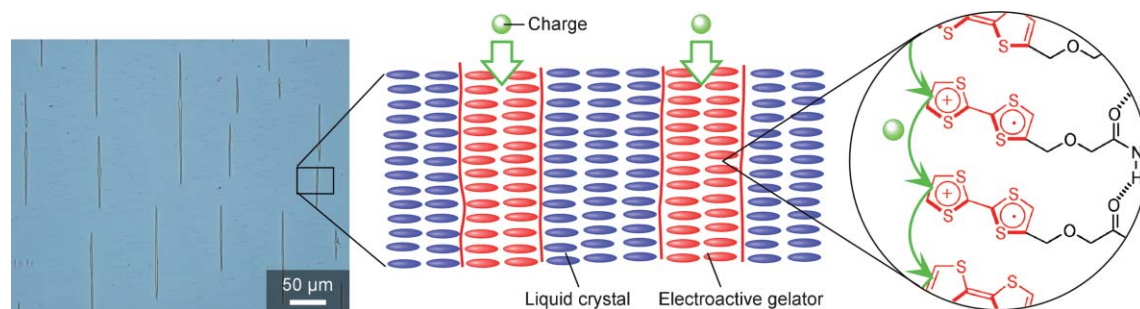


**Fig. 21** Photomicrographs and schematic illustration of the oriented hierarchical structure formed in the LC physical gels of **13** in the parallel rubbed cell.

gelators leads to the preparation of new functional materials such as electro-optical displays and organic electro-active materials. These induced or enhanced functions of LC physical gels are achieved by tuning the microphase-separated structures that are dependent on the combination of the liquid crystals and gelators. Moreover, the structures are thermally reversible. The structures can also be stabilised by using photopolymerisable gelators. These materials are new soft materials that have great potentials as stimuli-responsive functional materials.

## Acknowledgements

We would like to thank co-workers whose names appear in our cited references.

## References

- 1 *Polymer Gels*, ed. D. DeRossi, K. Kajiwara, Y. Osada and A. Yamaguchi, Plenum Press, New York, 1991.
- 2 *Low Molecular Mass Gelators*, ed. F. Fages, Springer, Berlin, 2005.
- 3 N. M. Sangeetha and U. Maitra, *Chem. Soc. Rev.*, 2005, **34**, 821.
- 4 S. Shinkai and K. Murata, *J. Mater. Chem.*, 1998, **8**, 485.
- 5 D. J. Abdallah and R. G. Weiss, *Adv. Mater.*, 2000, **12**, 1237.
- 6 K. Hanabusa, R. Tanaka, M. Suzuki, M. Kimura and H. Shirai, *Adv. Mater.*, 1997, **9**, 1095.
- 7 K. Hanabusa, H. Nakayama, M. Kimura and H. Shirai, *Chem. Lett.*, 2000, **29**, 1070.
- 8 K. Hanabusa, M. Yamada, M. Kimura and H. Shirai, *Angew. Chem., Int. Ed. Engl.*, 1996, **35**, 1949.
- 9 T. Brotin, R. Utermöhlen, F. Fages, H. Bousas-Laurent and J.-P. Desvergne, *J. Chem. Soc., Chem. Commun.*, 1991, 416.
- 10 *Handbook of Liquid Crystals*, ed. D. Demus, J. W. Goodby, G. W. Gray, H.-W. Spiess and V. Vill, Wiley-VCH, Weinheim, 1998.
- 11 *Thermotropic Liquid Crystals*, ed. G. W. Gray, Wiley, Chichester, 1987.
- 12 M. Schadt and W. Helfrich, *Appl. Phys. Lett.*, 1971, **18**, 127.
- 13 J. H. Haaren and D. Broer, *Chem. Ind.*, 1998, **1998**, 1017.
- 14 R. J. Bushby and O. R. Lozman, *Curr. Opin. Solid State Mater. Sci.*, 2003, **6**, 569.
- 15 *Liquid Crystals in Complex Geometries Formed by Polymer and Porous Networks*, ed. G. P. Crawford and S. Zumer, Taylor & Francis, London, 1996.
- 16 R. A. M. Hikmet, *Adv. Mater.*, 1992, **4**, 679.
- 17 S. M. Kelly, *J. Mater. Chem.*, 1995, **5**, 2470.
- 18 C. A. Guymon, E. N. Hoggan, N. A. Clark, T. P. Rieker, D. M. Walba and C. N. Bowman, *Science*, 1997, **275**, 57.
- 19 T. Kato, N. Mizoshita and K. Kishimoto, *Angew. Chem., Int. Ed. Engl.*, 2006, **45**, 38.
- 20 T. Kato, *Science*, 2002, **295**, 2414.
- 21 T. Kato, N. Mizoshita, M. Moriyama and T. Kitamura, *Top. Curr. Chem.*, 2005, **256**, 219.
- 22 T. Kato, N. Mizoshita and K. Kanie, *Macromol. Rapid Commun.*, 2001, **22**, 797.
- 23 T. Kato, T. Kutsuna, K. Hanabusa and M. Ukon, *Adv. Mater.*, 1998, **10**, 606.
- 24 T. Kato, G. Kondo and K. Hanabusa, *Chem. Lett.*, 1998, **27**, 193.
- 25 K. Yabuuchi, A. E. Rowan, R. J. M. Nolte and T. Kato, *Chem. Mater.*, 2000, **12**, 440.
- 26 N. Mizoshita, T. Kutsuna, K. Hanabusa and T. Kato, *Chem. Commun.*, 1999, 781.
- 27 T. Kato, T. Kutsuna, K. Yabuuchi and N. Mizoshita, *Langmuir*, 2002, **18**, 7086.
- 28 N. Mizoshita and T. Kato, unpublished work.
- 29 N. Mizoshita, K. Hanabusa and T. Kato, *Adv. Mater.*, 1999, **11**, 392.
- 30 N. Mizoshita, K. Hanabusa and T. Kato, *Adv. Funct. Mater.*, 2003, **13**, 313.
- 31 N. Mizoshita, Y. Suzuki, K. Kishimoto, K. Hanabusa and T. Kato, *J. Mater. Chem.*, 2002, **12**, 2197.
- 32 Y. Suzuki, N. Mizoshita, K. Hanabusa and T. Kato, *J. Mater. Chem.*, 2003, **13**, 2870.
- 33 X. Tong, Y. Zhao, B.-K. An and S. Y. Park, *Adv. Funct. Mater.*, 2006, **16**, 1799.
- 34 X. Tong and Y. Zhao, *J. Am. Chem. Soc.*, 2007, **129**, 6372.
- 35 N. Mizoshita, Y. Suzuki, K. Hanabusa and T. Kato, *Adv. Mater.*, 2005, **17**, 692.
- 36 M. Moriyama, N. Mizoshita, T. Yokota, K. Kishimoto and T. Kato, *Adv. Mater.*, 2003, **15**, 1335.
- 37 M. Moriyama, N. Mizoshita and T. Kato, *Bull. Chem. Soc. Jpn.*, 2006, **79**, 962.
- 38 M. Moriyama, N. Mizoshita and T. Kato, *Polym. J.*, 2004, **36**, 661.
- 39 Y. Zao and X. Tong, *Adv. Mater.*, 2003, **15**, 1431.
- 40 N. Mizoshita and T. Kato, *Adv. Funct. Mater.*, 2006, **16**, 2218.
- 41 N. Mizoshita, H. Monobe, M. Inoue, M. Ukon, T. Watanabe, Y. Shimizu, K. Hanabusa and T. Kato, *Chem. Commun.*, 2002, 428.
- 42 T. Kitamura, S. Nakaso, N. Mizoshita, Y. Tochigi, T. Shimomura, M. Moriyama, K. Ito and T. Kato, *J. Am. Chem. Soc.*, 2005, **127**, 14769.
- 43 K. Yabuuchi, Y. Tochigi, N. Mizoshita, K. Hanabusa and T. Kato, *Tetrahedron*, 2007, **63**, 7358.
- 44 C. Tolksdorf and R. Zentel, *Adv. Mater.*, 2001, **13**, 1307.
- 45 P. Deindörfer, A. Eremin, R. Stannarius, R. Davis and R. Zentel, *Soft Matter*, 2006, **2**, 693.
- 46 P. S. Dorzaic, *J. Appl. Phys.*, 1986, **60**, 2142.
- 47 J. W. Doane, N. A. Vaz, B.-G. Wu and S. Zumer, *Appl. Phys. Lett.*, 1986, **48**, 269.
- 48 T. Kajiyama, A. Miyamoto, H. Kikuchi and Y. Morimura, *Chem. Lett.*, 1989, **18**, 813.
- 49 M. C. W. van Boxtel, R. H. C. Janssen, D. J. Broer, H. T. A. Wilderbeek and C. W. M. Bastiaansen, *Adv. Mater.*, 2000, **12**, 753.
- 50 N. Boden, R. J. Bushby, J. Clements, B. Movaghar, K. J. Donovan and T. Kreouzis, *Phys. Rev. B*, 1995, **52**, 13274.
- 51 For recent examples: J. Sly, P. Kasák, E. Gomar-Nadal, C. Rovira, L. Górris, P. Thordarson, D. B. Amabilino, A. E. Rowan and R. J. M. Nolte, *Chem. Commun.*, 2005, 1255; B. W. Messmore, J. F. Hulvat, E. D. Sone and S. I. Stupp, *J. Am. Chem. Soc.*, 2004, **126**, 14452; T. Kitahara, M. Shirakawa, S. Kawano, U. Beginn, N. Fujita and S. Shinkai, *J. Am. Chem. Soc.*, 2005, **127**, 14980; C. Wang, D. Zhang and D. Zhu, *J. Am. Chem. Soc.*, 2005, **127**, 16372; K. Naka, D. Ando, X. Wang and Y. Chujo, *Langmuir*, 2007, **23**, 3450; M. Hasegawa, H. Enozawa, Y. Kawabata and M. Iyoda, *J. Am. Chem. Soc.*, 2007, **129**, 3072.
- 52 G. Saito and Y. Yoshita, *Bull. Chem. Soc. Jpn.*, 2007, **80**, 1.
- 53 J. L. Segura and N. Martín, *Angew. Chem., Int. Ed.*, 2001, **40**, 1372.
- 54 H. Hogel, *J. Phys. Chem.*, 1965, **69**, 755.